

# LOCALIZATION OF PLANAR ACOUSTIC REFLECTORS FROM THE COMBINATION OF LINEAR ESTIMATES

Jason Filos<sup>1</sup>, Antonio Canclini<sup>2</sup>, Fabio Antonacci<sup>2</sup>, Augusto Sarti<sup>2</sup> and Patrick A. Naylor<sup>1</sup>

<sup>1</sup> Electrical and Electronic Engineering,  
Imperial College London, UK  
email: {jason.filos, p.naylor}@imperial.ac.uk

<sup>2</sup> Dipartimento di Elettronica ed Informazione,  
Politecnico di Milano, Milano, Italy  
email: {canclini, antonacc, sarti}@elet.polimi.it

## ABSTRACT

In this paper we present a simple yet effective method for estimating the geometry of an acoustic enclosure in three-dimensions. By capturing the acoustic impulse responses using a microphone array and a loudspeaker at different spatial locations we transform the localization of planar reflectors into the estimation of multiple linear reflectors. By decomposing the microphone array into co-planar sub-arrays the line parameters of the reflectors lying on the corresponding planes can be inferred using a geometric constraint. By intersecting these lines the actual lying plane of each reflector can be estimated. The proposed method is evaluated using a three-dimensional microphone array in a real conference room.

## 1. INTRODUCTION

Knowledge of the geometry of a room can play an important role for many applications of space-time processing. Well-known examples are [1] and [2] where the authors demonstrate that a correct modelling of the reflections inside a room can improve the accuracy of the processing algorithms.

Many techniques have appeared in the last few years, which aim at localizing principal reflectors in a room. Relevant examples are [2–6]. All these techniques, however, are specialized to the estimation of two-dimensional (2-D) geometries. There are applications, however, where reflections from floor and ceiling are relevant and can affect the accuracy of the outcome of the space-time processing. In [7] the authors generalize the approach in [3,4] to three-dimensional (3-D) geometries. In this paper we start once again from the approach introduced in [3,4] but propose a rather different approach to the estimation of simple 3-D geometries, which transforms the localization of planar reflectors into the estimation of multiple linear reflectors. More specifically, we adopt a 3-D array accommodating seven microphones. Microphones are organized in three sub-arrays, each composed

of five microphones. All the microphones in a specific sub-array are characterized by the fact that they are co-planar. Each sub-array is devoted to the localization of the portion of reflectors lying on its plane. By intersecting line-reflectors estimated from multiple sub-arrays, the proposed methodology estimates the actual lying plane of each reflector.

An Acoustic Impulse Response (AIR) acquired in an ordinary room can be richly populated with peaks related to reflective paths, only some of which are related to first-order reflections. We consider these first-order echoes as the only acoustic events useful for the localization of reflectors. A preliminary step that selects only the useful acoustic events, i.e. the Times Of Arrival (TOAs) related to the direct-path propagation and the first-order reflective paths, is therefore necessary. For this purpose we propose a technique based on the Hough transform. The Hough transform for the detection of reflectors was first introduced in [8]. Based on the assumption that all the cartesian sections of the room are rectangular, we select the reflective paths in the impulse response which are organized on a rectangular pattern in the Hough parameter space. This rectangle detection technique is inspired by the solution to a similar problem adopted in computer vision [9]. It is worth noticing that this approach can be easily generalized to convex polygonal rooms [10].

## 2. SIGNAL MODEL

Let  $M$  sensors be distributed in a 3-D volume at positions  $\mathbf{r}_i \triangleq [x_i \ y_i \ z_i]^T$ ,  $i = 0, \dots, M - 1$ , and a source at  $\mathbf{r}_s \triangleq [x_s \ y_s \ z_s]^T$ . Each sensor receives the output signal given by

$$x_i(t) = \mathbf{h}_i^T \mathbf{s}(t) + b_i(t), \quad (1)$$

where  $\mathbf{h}_i$  is the  $i$ th channel acoustic impulse response,  $\mathbf{s}(t)$  the source signal at time  $t$  and  $b_i(t)$  is the additive noise at the  $i$ th output. This output is composed of the sum of the direct-path signal and scaled replicas of the source signal. The delay of each replica is determined by the respective positions of reflectors, source and receivers. Accordingly, the AIRs are

The authors acknowledge the financial support of the Future and Emerging Technologies (FET) programme within the Seventh Framework Programme for Research of the European Commission, under FET-Open grant number: 226007 SCENIC.

given by

$$h_i(t) = \sum_{q=0}^Q \alpha_{i,q} \delta(t - \tau_{i,q}), \quad (2)$$

where  $Q$  is the total number of reflections of all orders,  $\alpha_{i,q}$  is an attenuation term and  $\tau_{i,q}$  is defined as the TOA associated with the  $i$ th sensor and the  $q$ th reflection. In vector/matrix form the model is expressed as

$$\mathbf{x}(t) = \mathbf{H}\mathbf{s}(t) + \mathbf{b}(t), \quad (3)$$

where

$$\begin{aligned} \mathbf{x}(t) &= [x_0(t) \ x_1(t) \ \cdots \ x_{M-1}(t)]^T, \\ \mathbf{H} &= \begin{bmatrix} h_{0,0} & h_{0,1} & \cdots & h_{0,L-1} \\ h_{1,0} & h_{1,1} & \cdots & h_{1,L-1} \\ \vdots & \vdots & \ddots & \vdots \\ h_{M-1,0} & h_{M-1,1} & \cdots & h_{M-1,L-1} \end{bmatrix}_{M \times L}, \\ \mathbf{s}(t) &= [s(t) \ s(t-1) \ \cdots \ s(t-L+1)]^T, \\ \mathbf{b}(t) &= [b_0(t) \ b_1(t) \ \cdots \ b_{M-1}(t)]^T, \end{aligned}$$

and  $L$  is the length of the longest channel impulse response. Let  $N$  denote the amount of first-order reflections. For every  $i$ th sensor we define  $\boldsymbol{\tau}_i = [\tau_{i,0} \ \tau_{i,1} \ \cdots \ \tau_{i,N}]^T$  as the vector containing the direct-path TOA along with the  $N$  first-order reflective path TOAs in discrete time.

### 2.1. Geometrical Considerations

Given the signal model introduced in Section 2 it is desirable to populate  $\boldsymbol{\tau}_i$ , containing the full set of TOAs for all channels, using a one-shot acquisition, i.e. by probing the acoustic environment from only one source position at one point in time. The authors in [5] interestingly claim that it is possible to reconstruct the geometry of an acoustic enclosure from a single AIR. While this is indeed true for most convex polygonal geometries there are certain modelling assumptions that are not fully satisfiable. First and foremost, and in contrast to this manuscript, the authors consider not only first-order reflections but also second-order echoes. It is relatively straightforward to see that if an obtuse angle is present in the geometry of the enclosure it is impossible to obtain second-order reflections from that pair of walls using a collocated microphone and source.

Although the method adopted in [5] is unique and approaches the problem of geometric inference in a mathematical elegant way, it assumes a full set of TOAs in the AIR that contains the direct-path, first and second-order echoes. While such a set is straightforward to obtain in simulation, it is often impossible in real reverberant environments. This is mainly due to the fact that a sound source, such as a loudspeaker, does not exhibit an ideal omnidirectional directivity pattern but also because of other effects such as occlusion, non-ideal reflectivity of the building materials and interference.

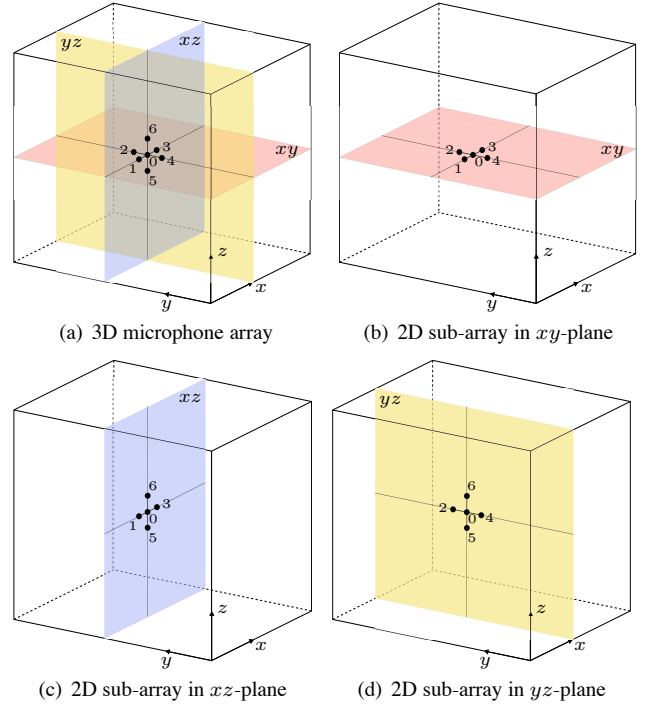


**Fig. 1:** 7-element microphone array inside a room: Full 3D array (a) and decomposition into three 2D sub-arrays (b)–(d).

### 3. PROPOSED METHOD

In this paper, we aim to obtain the full TOA set  $\boldsymbol{\tau}_i$ , i.e. the set that allows the identification of all reflectors (i.e. walls) that define the boundaries of the acoustic enclosure, by considering multiple source positions. This is achieved by acquiring  $\mathbf{H}$  at different source locations. We define the varying spatial positions of the source as  $\mathbf{r}_u \triangleq [x_u \ y_u \ z_u]^T$ ,  $u = 0, \dots, N-1$ . At each step the multi-channel impulse response,  $\mathbf{H}_u$ ,  $u = 0, \dots, N-1$ , is identified. The vector  $\boldsymbol{\tau}_i$  is obtained from the matrix  $\mathbf{H}_u$  by picking the peaks of the columns of  $\mathbf{H}_u$ , containing the impulse responses from  $\mathbf{r}_u$  to each microphone in the array. For further details on the peak picking the interested reader can refer to [4].

In this work, two limitations are considered. First, the number of source positions,  $N$ , is chosen a priori to correspond to the total number of reflectors present in the environment. Secondly, the source is placed in a favourable position at each step, meaning that the first two peaks in  $\mathbf{H}_u$  always correspond to the direct-path and first-order reflection, with respect to each particular source position, microphone array and reflector arrangement. Evidently,  $\mathbf{H}_u$  contains information related to more than one reflector. Exploiting such redundancy is indeed possible, such as proposed by the authors in [4]. However, for the purposes of this paper we do not aim at exploiting redundancy or the reduction of the amount of source positions probed.

The 2-D reflector localization techniques outlined in [3,

4,8] are extended to the 3-D case in a straightforward yet effective way. A 3-D microphone array, such as depicted in Figure 1(a), is employed to capture  $\mathbf{H}_u$ . The 3-D space is decomposed into three orthogonal 2-D regions by considering three subsets of microphones. Let  $\mathbf{r}_{xy}$ ,  $\mathbf{r}_{xz}$ ,  $\mathbf{r}_{yz}$  denote the subsets lying on the  $xy$ ,  $xz$  and  $yz$ -planes, as shown in Figures 1(b)–1(d) respectively. Each subset is used to identify the line parameters of the reflectors coincident with the plane it can *see*. By combining the measurements from all three planes we observe that each reflector plane is represented by a pair of lines lying on two orthogonal planes. By first estimating the line parameters of the reflectors it is possible to then calculate the parameters of the planes that are coincident with the actual reflectors in 3-D. In the following Section we will outline the estimation of the line parameters of the reflectors followed by the reflector plane estimation methodology.

#### 4. REFLECTOR LINE ESTIMATION

Given the geometric inference framework introduced in [3,4] we define, in homogenous coordinates, a conic in two dimensions using parameters  $\{a, b, c, d, e, f\}$  as

$$\mathcal{C} = \{(x, y) \in \mathbb{R}^2 | ax^2 + 2bxy + cy^2 + 2dx + 2ey + f = 0\}. \quad (4)$$

By setting  $\mathbf{x} = [x \ y \ 1]^T$  and  $\mathbf{C} = \begin{bmatrix} a & b & d \\ b & c & e \\ d & e & f \end{bmatrix}$  this can

be written  $\mathbf{x}^T \mathbf{C} \mathbf{x} = 0$ . The ellipse associated with the  $i$ th microphone, ( $i \in \{0, \dots, M-1\}$ ), and the  $k$ th reflector, ( $k \in \{1, \dots, N\}$ ), is defined as  $\mathbf{C}_{i,k}$ . The estimation of the unknown parameters of  $\mathbf{C}_{i,k}$  is outlined in detail in [4]. Furthermore a line in homogeneous coordinates is expressed as

$$\mathcal{L} = \{(x, y) \in \mathbb{R}^2 | l_1 x + l_2 y + l_3 = 0\}, \quad (5)$$

which after setting  $\mathbf{l} = [l_1 \ l_2 \ l_3]^T$  can be written as  $\mathbf{l}^T \mathbf{x} = 0$ . If we group together  $M$  ellipses that are associated with a particular reflector, then its line parameters can be estimated using the following cost function:

$$J(\mathbf{l}, \{\mathbf{C}_{i,k}^*\}_{i=0}^{M-1}) = \sum_{i=0}^{M-1} \|\mathbf{l}^T \mathbf{C}_{i,k}^* \mathbf{l}\|^2, \quad (6)$$

where  $M \geq 3$  and  $\mathbf{C}_{i,k}^* = \det(\mathbf{C}_{i,k}) \mathbf{C}_{i,k}^{-1}$  is the adjoint of the conic-matrix  $\mathbf{C}_{i,k}$ . The cost function in (6), a nonlinear and non-convex function, can be solved using least-squares [4] or using an analytic method based on a closed-form estimator [8]. For every subset  $\mathbf{r}_{xy}$ ,  $\mathbf{r}_{xz}$ ,  $\mathbf{r}_{yz}$  the TOA information,  $\tau_i$ , along with the current source position,  $\mathbf{r}_u$ , and the geometry of the sub-array from  $\mathbf{r}_i$ , are used to construct the ellipses that yield the line parameters of the reflectors.

#### 4.1. Disambiguation of TOA Information

The vectors  $\tau_i$  contain TOA information related to all first-order reflections. Since we decompose the 3-D problem geometry into three orthogonal 2-D planes, it follows that there are elements in the vector  $\tau_i$  of each channel that are not related to the TOAs associated with the reflectors of a particular plane. Since only the TOAs that are relevant to a particular plane yield the correct line parameters there exists an ambiguity problem in the choice of elements from  $\tau_i$ .

Consider a rectangular room like in Figure 1(a). Assuming only first-order reflections each microphone will capture, apart from the direct-path TOA, six additional TOAs. However, only four TOAs are relevant for every sub-array. Disambiguation of TOA information is an ongoing area of research. Existing methods, such as [11], can be used and adapted to the framework of this paper. However, following on the theoretical framework presented in our previous contribution to this conference in [8] and due to space limitations, we will only hint at disambiguations of TOA information in the AIRs in this paper, and leave out the algorithmic details to a forthcoming extended version of this paper.

In [8] we outlined a method that works out a number of coordinate points based on the line parameters of a reflector  $\mathbf{l}$ . By using the Hough transform and by considering multiple source positions  $\mathbf{r}_u$ , we showed how to improve the numerical accuracy of  $\mathbf{l}$ . In this manuscript we adopt a similar framework. Given  $M$  microphones and  $N$  source positions, we define

$$\xi_j \triangleq [x_j \ y_j]^T, \quad j = 0, \dots, P, \quad (7)$$

where  $MN - 1 \leq P \leq 2MN - 1$ , as a collection of coordinate points that satisfy certain geometrical relationships, enumerated in [8], between ellipses and reflector lines. The aim is to obtain a representation of the reflectors in the Hough transform domain in order to aid in the disambiguation of TOA information. We note that the coordinate points in  $[\xi_0 \ \xi_1 \ \dots \ \xi_P]$  are obtained after the line parameters of a reflector have been estimated. We would like to point out that these coordinate points can be calculated directly from  $\tau_i$ , but for the sake of coherency with our previous work we adopt the same geometrical framework based on ellipses and lines.

#### 4.2. Disambiguation of rectangular patterns in the Hough transform domain

The Hough transform can be used for estimating the parameters of a shape from its boundary points [12]. It considers the following normal parametrization

$$\rho = x \cos \theta + y \sin \theta, \quad (8)$$

which specifies a straight line by the angle  $\theta$  of its normal and its algebraic distance  $\rho$  from the origin. A point in the cartesian space maps to a sinusoid in the Hough parameter

space that corresponds to all the lines passing through it. Conversely, points in the parameter space are transformed into lines in the Cartesian coordinate space. Given two points lying on a line with parameters  $\rho, \theta$ , in the Hough parameter space the sinusoids corresponding to these two points intersect at  $\rho, \theta$ . Therefore, given the points  $\xi_j$  in the coordinate space, the parameters of a line corresponding to the best-fit of  $\xi_j$  can be found. Let  $\rho \in \mathbb{R}$  and  $\theta \in [0, \pi]$ . For each point  $[x_j \ y_j]^T$  we calculate

$$\hat{\rho} = x_j \cos \hat{\theta} + y_j \sin \hat{\theta}. \quad (9)$$

The results are stored in an accumulator  $\mathcal{A}$ , initially set to zero, which is incremented at every step such that:

$$\mathcal{A}(\hat{\rho}, \hat{\theta}) = \mathcal{A}(\hat{\rho}, \hat{\theta}) + 1. \quad (10)$$

The accumulator space  $\mathcal{A}$  is defined over a grid of points. The resolution of the grid influences the accuracy of the peak detection. In our experiments we have used a resolution of 0.5 mm and  $0.25^\circ$ , with a range of 4 meters. Let  $H_1 = (\rho_1, \theta_1), H_2 = (\rho_2, \theta_2), \dots, H_v = (\rho_v, \theta_v)$  denote the  $v$  peaks of  $\mathcal{A}(\hat{\rho}, \hat{\theta})$  [9]. Peaks  $H_m$  and  $H_n$  are paired together if they satisfy:

$$|\theta_m - \theta_n| \approx T_\theta, \quad (11)$$

where  $T_\theta$  is an angular threshold, and determines if peaks  $H_m$  and  $H_n$  correspond to orthogonal lines (i.e.  $T_\theta \approx \pi/2$ ).

For every microphone sub-array the peaks in the accumulator are sorted with respect to (11). In this way elements in  $\tau_i$  that are not related to a particular sub-array, and its respective plane, can be discarded. For the purposes of this paper we only consider rectangular geometries. We would like to refer to [10] and point out that it is possible to form other geometrical relationships in order to perform disambiguation in more complex geometries.

## 5. REFLECTOR PLANE ESTIMATION

The estimation process outlined in the previous Section leads to 6 pairs of reflector lines, one pair for each wall. In particular, each wall is represented by a pair of lines lying on two orthogonal planes. In theory, these lines are incident, and the reflector is easily found as the plane containing them. In practice, however, estimation errors may cause the two lines to be skew. The reflector, therefore, has to be estimated as the plane which best fits the two lines.

We proceed as follows. With reference to Fig. 2, let us consider two arbitrary skew lines  $l_1$  and  $l_2$ . We aim at estimating the plane  $\mathbf{P} = [\mathbf{n}, d]^T$  that best fits  $l_1$  and  $l_2$ , where the unit vector  $\mathbf{n}$  is the normal of the plane, and  $d$  is its distance from the origin. For each line we select two arbitrary points lying on it, namely  $\mathbf{p}_1$  and  $\mathbf{q}_1$  on  $l_1$ ; and  $\mathbf{p}_2$  and  $\mathbf{q}_2$  on

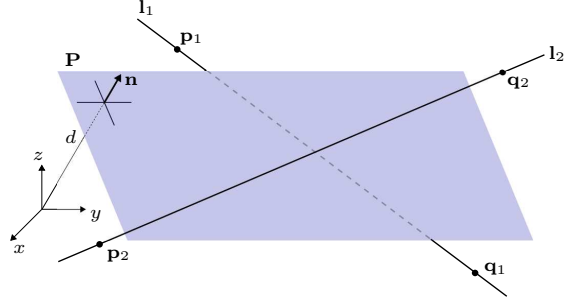


Fig. 2: Plane estimation from two skew lines.

$l_2$ . We organize the point coordinates in the matrix

$$\mathbf{G} = \begin{bmatrix} \mathbf{p}_1 & 1 \\ \mathbf{q}_1 & 1 \\ \mathbf{p}_2 & 1 \\ \mathbf{q}_2 & 1 \end{bmatrix}. \quad (12)$$

The searched plane is then estimated, in the least-squares sense, as

$$\hat{\mathbf{P}} = [\hat{\mathbf{n}}, \hat{d}]^T = \underset{\mathbf{n}, d}{\operatorname{argmin}} \|\mathbf{G}[\mathbf{n}, d]^T\|^2 \quad \text{s.t.} \quad \|\mathbf{n}\| = 1. \quad (13)$$

## 6. EXPERIMENTAL VERIFICATION

The accuracy of the system has been tested in a real room measuring  $L \times W \times H = 2.77\text{m} \times 3.55\text{m} \times 3.17\text{m}$ , built with concrete walls and ceiling and floored with linoleum panels. The central microphone of the array is placed at a distance of 1.2m from the West wall, 1.91m from the South wall and 1.59m from the floor. The array is composed of 7 omnidirectional microphones. On the horizontal plane the extension of the array is  $0.5\text{m} \times 0.5\text{m}$ , while the microphones on the vertical axis are kept 0.38cm apart. A loudspeaker placed at 6 different spatial locations emits an MLS sequence sampled at 48kHz and acquired at the same frequency. The sequence is then processed to extract the impulse response from each position of the source to each microphone in the array.

The accuracy of the reflector localization is assessed in two steps. First the estimated line parameters in each of the three planes are compared to the hand measured ground truths in terms of a distance and angular error. As a next step the estimated plane parameters are compared to the true planes in terms of a point-plane distance and their dihedral angle.

Let  $l$  and  $\hat{l}$  be the reflector line and its estimate, respectively. From these we can evaluate the distance  $D_{2D}$  from  $\mathbf{r}_0$  to each line and the orientation  $A_{2D}$ . The distance and orientation can be evaluated by projecting  $\mathbf{r}_0$  onto the line such that  $D_{2D} = \frac{|l_1 x_0 + l_2 y_0 + l_3|}{\sqrt{l_1^2 + l_2^2}}$ ,  $A_{2D} = \arctan \frac{l_2}{l_1}$ . The accuracy of the reflector localization is measured in terms of distance error  $\epsilon_d = |D_{2D} - \hat{D}_{2D}|$  and angular error  $\epsilon_a = |A_{2D} - \hat{A}_{2D}|$ . The distance and angular error results for the reflector lines in 2-D are shown for the  $xy, xz$  and  $yz$  planes in table 1.

**Table 1:** Distance and angular error results in each plane

Reflector	$xy$		$xz$		$yz$	
	$\epsilon_d$ [cm]	$\epsilon_a$ [°]	$\epsilon_d$ [cm]	$\epsilon_a$ [°]	$\epsilon_d$ [cm]	$\epsilon_a$ [°]
West	1.180	0.619	2.720	0.871		
South	1.030	1.598			4.810	0.034
East	1.310	0.160	7.300	0.504		
North	1.690	0.160			3.100	0.756
Ceiling			1.620	0.728	2.780	0.275
Floor			1.030	1.598	0.210	0.092

**Table 2:** Distance and angular error comparison in 3-D

Reflector	$\epsilon_D$ [cm]	$\Phi$ [°]
West	0.260	1.068
South	1.300	0.718
East	7.950	0.528
North	0.063	0.773
Ceiling	1.050	1.601
Floor	3.860	0.778

Let  $\mathbf{P}$  and  $\hat{\mathbf{P}}$  be the true and estimated reflector planes respectively. From these we can evaluate the distance  $D_{3D}$  from  $\mathbf{r}_0$  to each plane (point-plane distance) and the angle  $A_{3D}$  between true and estimate planes (dihedral angle). The distance is given by  $D_{3D} = \mathbf{n}^T [x_0 \ y_0 \ z_0] + d$ , where  $\mathbf{n}$  is the unit normal vector of  $\mathbf{P}$ , and  $d$  is the constant of the Hessian normal form. The distance error is calculated as  $\epsilon_D = |D_{3D} - \hat{D}_{3D}|$  and the dihedral angle is given by  $\Phi = \arccos(\mathbf{n}^T \hat{\mathbf{n}})$ . The results for the plane localization in 3-D are shown in table 2.

### 6.1. Results and Discussion

The localization method estimates, both in 2-D and 3-D, the real reflector positions in the environment with high accuracy. It is important to note however that errors propagate directly from the estimation of the linear reflectors to the localization of the planar reflectors. The experiment in a real conference room serves as an exemplar in this manuscript to outline the applicability of the proposed method to 3-D geometries. A more robust system identification and source range estimation, such as in [4], should be employed in conjunction with this method when higher localization accuracy is desired.

## 7. CONCLUSIONS

We presented an approach for estimating the geometry of an acoustic enclosure in three-dimensions by transforming the localization of planar reflectors into the estimation of multiple linear reflectors. Experimental results in a real conference room demonstrate the feasibility of the proposed method.

## 8. REFERENCES

- [1] T. Betlehem and T.D. Abhayapala, "Theory and design of sound field reproduction in reverberant rooms," *J. Acoust. Soc. Amer.*, vol. 117, pp. 2100–2111, 2005.

- [2] D. Ba, F. Ribeiro, Cha Zhang, and D. Florêncio, "L1 regularized room modeling with compact microphone arrays," in *Proc. IEEE Intl. Conf. on Acoustics, Speech and Signal Processing (ICASSP)*, Dallas, Tx, Mar. 2010, pp. 157–160.
- [3] F. Antonacci, A. Sarti, and S. Tubaro, "Geometric reconstruction of the environment from its response to multiple acoustic emissions," in *Proc. IEEE Intl. Conf. on Acoustics, Speech and Signal Processing (ICASSP)*, Dallas, Tx, Mar. 2010, pp. 2822–2825.
- [4] J. Filos, E. A. P. Habets, and P. A. Naylor, "A two-step approach to blindly infer room geometries," in *Proc. Intl. Workshop Acoust. Echo Noise Control (IWAENC)*, Tel Aviv, Israel, Sept. 2010.
- [5] I. Dokmanic, Y. Lu, and M. Vetterli, "Can One Hear the Shape of a Room: The 2D Polygonal Case," in *Proc. IEEE Intl. Conf. on Acoustics, Speech and Signal Processing (ICASSP)*, Prague, Czech Republic, May 2011, pp. 321–324.
- [6] S. Tervo and T. Korhonen, "Estimation of reflective surfaces from continuous signals," in *Proc. IEEE Intl. Conf. on Acoustics, Speech and Signal Processing (ICASSP)*, Dallas, Tx, Mar. 2010, pp. 153–156.
- [7] E. Nastasia, F. Antonacci, A. Sarti, and S. Tubaro, "Localization of planar acoustic reflectors through emission of controlled stimuli," in *Proc. European Signal Processing Conf. (EUSIPCO)*, Barcelona, Spain, Aug. 2011.
- [8] J. Filos, A. Canclini, M. R. P. Thomas, F. Antonacci, A. Sarti, and P. A. Naylor, "Robust inference of room geometry from acoustic impulse responses," in *Proc. European Signal Processing Conf. (EUSIPCO)*, Barcelona, Spain, Aug. 2011.
- [9] C.R. Jung and R. Schramm, "Rectangle detection based on a windowed Hough transform," in *Computer Graphics and Image Processing, 2004. Proceedings. 17th Brazilian Symposium on*, Oct. 2004, pp. 113–120.
- [10] A. Rosenfeld and I. Weiss, "A convex polygon is determined by its Hough transforms," *Pattern Recogn. Lett.*, vol. 16, no. 3, pp. 305–306, Mar. 1995.
- [11] J. Scheuing and B. Yang, "Disambiguation of TDOA estimation for multiple sources in reverberant environments," *IEEE Trans. Speech Audio Process.*, vol. 16, no. 8, pp. 1479–1489, Nov. 2008.
- [12] Richard O. Duda and Peter E. Hart, "Use of the Hough transformation to detect lines and curves in pictures," *Commun. ACM*, vol. 15, pp. 11–15, 1972.